

A Monte Carlo Approach for the Cook-Torrance Model^{*}

I.T. Dimov, T.V. Gurov, and A.A. Penzov

Inst. for Par. Proc. - Bulg. Acad. of Sci.,
Acad. G. Bonchev st, bl. 25 A, 1113 Sofia, Bulgaria,
ivdimov@bas.bg
{gurov, apenzov}@parallel.bas.bg

Abstract. In this work we consider the rendering equation derived from the illumination model called Cook-Torrance model. A Monte Carlo (MC) estimator for numerical treatment of the this equation, which is the Fredholm integral equation of second kind, is constructed and studied.

1 Introduction

Photorealistic image creation is the main task in the area of computer graphics. The classical Radiosity and Ray Tracing algorithms have been developed to solve the global illumination for diffuse and specular scenes, respectively. However, application of these algorithms to general environments with multiple non-ideal reflection is restricted [8], due to local illumination model usage for image calculation. Monte Carlo algorithms provide with a proper rule for global illumination estimation of a scene, where the light radiated from the light sources is propagated through the scene objects to the human eye.

In order to estimate the global illumination in the scene, it is required to apply a suitable illumination model. The illumination model (see [14] for a survey of illumination models) describes the interaction of the light with a point on the surface in the scene. The simplest illumination model is independent of viewer direction and applicable for perfectly diffuse light reflecting scenes. It considers the light reflection as a sum of two components: ambient and Lambertian diffuse, reflecting light equally in all directions. In 1975 Phong [7] introduces an empirical three-component model with adding to illumination a new specular reflecting component. For the calculation of specular part, the viewer direction becomes more significant.

The first physical based illumination has been developed by Blinn [1] in 1977. And after that in 1982 Cook and Torrance [2] have suggested the complete implementation of the illumination model based on closer look to the physics of a surface. Cook-Torrance illumination model is an isotropic model and considers

* Supported by the EC through SEE-GRID project grant # RI-2002-002356 and by the NSF of Bulgaria through grant # I-1201/02.

the geometry of object surface to be non-ideally smooth but as composed of many microfacets. The microfacet surfaces are V shaped grooves where some microfacets shadow or mask each other. This fact leads up to some attenuation of reflected light. The roughness of the surface is defined by the microfacet distribution. Surface reflectance is described by Fresnel term of a single microfacet and may be obtained theoretically from the Fresnel equations [13].

Many others physical based illumination models develop and/or extend the Cook-Torrance model. An extension presented in [4] splits the diffuse reflection component into directional-diffuse and uniform-diffuse components. Anisotropic model of Ward [9] extends the scope of physical based illumination models. The physical illumination models are also applicable for photorealistic rendering when transparent objects exist in the scene [3].

Further in this paper we consider basically Cook-Torrance illumination model at construction of the Monte Carlo estimator for photorealistic image creation.

2 Rendering with Cook-Torrance Illumination Model

The goal of rendering is to calculate an image from a described 3D scene model. Photorealistic rendering requires realistic description of the scene model with accounting all physical characteristics of the surfaces and environment. The scene model consists of numerical definition of all objects and light sources in the scene, as well the virtual camera from which the scene is observed. Colours in computer graphics are frequently simulated in the RGB colour space, so the radiance $L = (r, g, b)$, where r , g , and b are the intensities for the selected wavelenghts of primary monitor colours (red, green and blue).

2.1 Basic Assumptions

The objects represent real physical objects including solid light sources like lamps with arbitrary defined position and orientation in the scene space. Usually the real solid objects are well modeled by approximation with planar surface primitives like triangles or rectangles. The number M of all surface primitives A_j is very large to ensure good object approximation for realistic rendering. Since the objects are independent scene units the scene domain, $S = \bigcup_{j=1}^M A_j$, is union of disjoint two-dimensional surface primitives A_j . The physical properties like reflectivity, roughness, and colour of the surface material are characterized by the bidirectional reflectance distribution function (BRDF), f_r . This function describes the light reflection from a surface point as a ratio of outgoing to incoming light. It depends on the wavelength of the light, incoming, outgoing light directions and location of the reflection point. The BRDF expression receives various initial values for the objects with different material properties. The same values for the BRDF expression are assigned to all surface primitives with equal material characteristics in the scene. Therefore, the number of surfaces with different material properties in the scene is m and the inequality $1 \leq m \leq M$ is hold.

The light sources can be both point light sources or solid light sources. The point light sources are defined by own position in the scene space and radiate light equally to all directions. The solid light sources are treated like ordinary scene objects itself radiating light. The total light intensity of solid light sources is distributed equally in a characteristic set of points generated on its surface and each point is considered like point light source.

The virtual camera frequently is assumed to be a pinhole camera and defines the eye view point position x_{eye} and orientation of scene observation. The image window situated in the projection plane of the camera is divided into matrix of rectangular elements and corresponds to the pixel matrix of the image to be generated. In order to generate an image, we have to calculate the radiance \bar{L}_P propagated in the scene and projected on each pixel area P in the image pixel matrix. This radiance value is radiated through the pixel area P into the eye view point x_{eye} . The radiance \bar{L}_P is mean value integral:

$$\bar{L}_P = \frac{1}{|P|} \int_P L(x_{eye}, x_p) dx_p \quad (1)$$

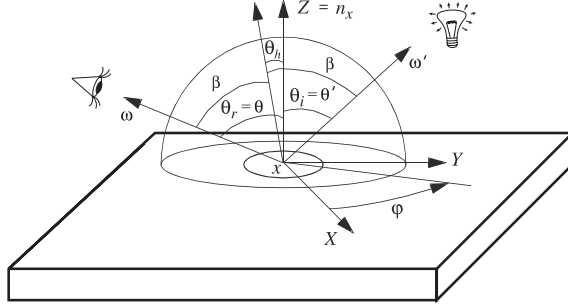
where $L(x_{eye}, x_p)$ is the radiance incoming from the nearest scene point $x \in S$ seen from the eye view point x_{eye} through the pixel position x_p into direction of the eye view point x_{eye} .

2.2 Rendering Equation by Cook-Torrance BRDF

The light propagation in a scene is described by rendering equation [5], which is a second kind Fredholm integral equation. According to Keller indications in [6], the radiance L , leaving from a point $x \in S$ on the surface of the scene in direction $\omega \in \Omega_x$, where Ω_x is the hemisphere in point x , is the sum of the self radiating light source radiance L^e and all reflected radiance:

$$L(x, \omega) = L^e(x, \omega) + \int_{\Omega_x} L(h(x, \omega'), -\omega') f_r(-\omega', x, \omega) \cos \theta' d\omega', \quad (2)$$

or in an operator form $L = L^e + \mathcal{K}L$. Here $y = h(x, \omega') \in S$ is the first point that is hit when shooting a ray from x into direction ω' and determines the objects visibility in the scene (see Fig. 1). The radiance L^e has non-zero value if the considered point x is a point from solid light source. Therefore, the reflected radiance in direction ω is an integral of the radiance incoming from all points, which can be seen through the hemisphere Ω_x in point x attenuated by the surface BRDF $f_r(-\omega', x, \omega)$ and the projection $\cos \theta'$, which puts the surface $S \times \Omega \rightarrow \mathbb{R}^+$ perpendicular to the ray (x, ω') . The angle θ' is the angle between surface normal in x and the direction ω' . The transport operator is physically correct when $\|\mathcal{K}\| < 1$, because a real scene always reflects less light than it receives from the light sources due to light absorption of the objects. The law for energy conservation holds, i.e.: $\alpha(x, \omega) = \int_{\Omega_x} f_r(-\omega', x, \omega) \cos \theta' d\omega' < 1$. That means the incoming photon is reflected with a probability less than 1,

**Fig. 1.** The geometry for the rendering equation

because the selected energy is less than the total incoming energy. Another important property of the BDRF is the Helmholtz principle: the value of the BRDF will not change if the incident and reflected directions are interchanged, $f_r(-\omega', x, \omega) = f_r(-\omega, x, \omega')$. In the terms of the Cook-Torrance illumination model [2], the BRDF is sum of diffuse $f_{r,d}$ and specular $f_{r,s}$ components:

$$f_r(-\omega', x, \omega) = f_{r,d}(x) + f_{r,s}(-\omega', x, \omega) = \frac{1}{\pi} \left(F(\lambda, \theta' = 0) + \frac{F(\lambda, \theta') D(\theta_h) G}{\cos \theta \cos \theta'} \right),$$

where the angle θ is the angle between surface normal in x and the direction ω . The microfacets distribution function is denoted by $D(\theta_h)$ and $G(\theta_h, \beta, \theta, \theta')$ is geometrical attenuation factor. Fresnel function $F(\lambda, \theta')$ depends on the wavelength λ , incident angle θ' of the light in point x , index of refraction, and absorption coefficient of surface material (see [13]). The diffuse part $f_{r,d}(x)$ of BRDF is the fraction of reflected radiance, independently of incoming and outgoing directions, and may be calculated from the Fresnel equations at angle of incident light $\theta' = 0$, or $f_{r,d}(x) = \frac{F(\lambda, \theta'=0)}{\pi}$. Both values of the microfacets distribution function $D(\theta_h)$ and the geometrical attenuation factor $G(\theta_h, \beta, \theta, \theta')$ are positive and can not exceed a maximum value of 1 (see [1]) in any real scene situation. Therefore, the specular part $f_{r,s}(-\omega', x, \omega)$ of BRDF reaches the maximum value when the Fresnel spectral term has absolute maximum for some light wavelength.

2.3 Analysis of the Neumann Series

Consider the *first-order stationary linear iterative process* for Eq. (2).

$$L_i = \mathbb{K} L_{i-1} + L^e, \quad i = 1, 2, \dots, \quad (3)$$

where i is the number of the iterations. In fact (3) defines a Neumann series

$$L_i = L^e + \mathbb{K} L^e + \dots + \mathbb{K}^{i-1} L^e + \mathbb{K}^i L_0, \quad i > 0,$$

where \mathbb{K}^i means the i -th iteration of the integral operator. If \mathbb{K} is a contraction, then $\lim_{i \rightarrow \infty} \mathbb{K}^i L_0 = 0$. Thus $L^* = \sum_{i=0}^{\infty} \mathbb{K}^i L^e$. If $i = k$ and $L_0 = 0$, one can get the value of the truncation error, namely, $L_k - L^* = \sum_{i=k}^{\infty} \mathbb{K}^i L^e$.

It is clear that every iterative algorithm uses a finite number of iterations k . In the presented MC approach below, we evaluate the iterations L_i , $1 \leq i \leq k$ with an additional statistical error. In practice the truncation parameter k is not a priori given. To define it let us denote $\|IK\|_{\mathbb{L}_1} = \max_{x,\omega} |\alpha(x,\omega)| = q < 1$ and $\|L^e\|_{\mathbb{L}_1} = L_*^e$. Further, in order to estimate the error we have

$$\|L_k - L^*\|_{\mathbb{L}_1} \leq L_*^e q^k \frac{1}{1-q}$$

Finally, to obtain a desired truncation error ε we have to select $k_\varepsilon = \min\{k \geq c_1 |\ln \varepsilon| + c_2\}$, where $c_1 = 1/|\ln(q)|$ and $c_2 = |\ln((1-q)/(L_*^e))|/|\ln(q)|$. In other cases the iteration parameter is obtained from the following condition: the difference between the stochastic approximation of two successive approximations has to be smaller than the given sufficiently small parameter ε .

3 A Monte Carlo Approach

Consider the problem for evaluating the following functional:

$$J_g(L) = (g, L) = \int_S \int_{\Omega_x} g(x, \omega) L(x, \omega) dx d\omega. \quad (4)$$

The radiance $L(., .) : S \times \Omega \rightarrow \mathbb{R}^+$ and the arbitrary function $g(., .) : S \times \Omega \rightarrow \mathbb{R}^+$ belong to the spaces \mathbb{L}_1 and \mathbb{L}_∞ , respectively. The case when $g(x, \omega) = \frac{\chi_P(x)}{|P|} \delta(\omega)$ is of special interest, because we are interested in computing the mean value of the radiance \bar{L}_P over pixel area (1). Here $\chi_P(x) = 1$ when $x \in P$, and $\chi_P(x) = 0$, otherwise. $\delta(\omega)$ is the Dirac delta-function. Since the Neumann series of the integral equation (2) converges, the functional (4) can be evaluated by a MC method. Let us introduce the following notation: $\omega'_0 = \omega_p$, $x_0 = x_p$, $x_1 = h(x_0, -\omega'_0)$, $x_2 = h(x_1, -\omega'_1)$, $x_3 = h(x_2, -\omega'_2) = h(h(x_1, -\omega'_1), -\omega'_2)$, ..., and define the kernels: $K(x_j, \omega'_j) = f_r(\omega'_j, x_j, \omega'_{j-1}) \cos \theta'_j$, $j = 1, 2, \dots, k_\varepsilon$. Consider a terminated Markov chain $(x_0, -\omega'_0) \rightarrow \dots \rightarrow (x_j, -\omega'_j) \rightarrow \dots \rightarrow (x_{k_\varepsilon}, -\omega'_{k_\varepsilon})$, such that $(x_j, -\omega'_j) \in S \times \Omega_x$, $j = 1, 2, \dots, k_\varepsilon$ (see Fig. 2). The initial point

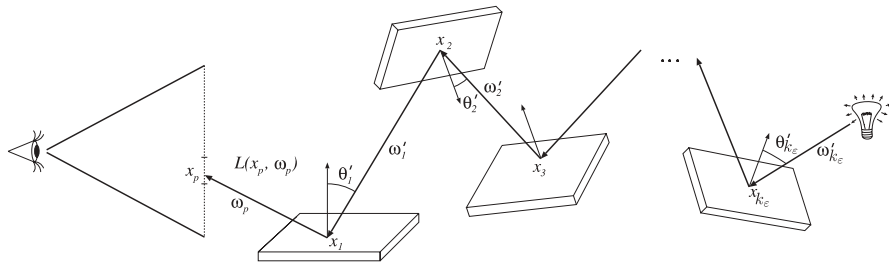


Fig. 2. One simulation of the terminated Markov chain

$(x_0, -\omega'_0)$ is chosen with an initial density $p_0(x, \omega')$. The other points are sampled using an arbitrary transition density function $p(x, \omega')$ which is tolerant (see definition in [10]) to the kernel in equation (2). The biased MC estimator for evaluating the functional (4) has the following form:

$$\xi_{k_\varepsilon}[g] = \frac{g(x_0, \omega'_0)}{p_0(x_0, \omega'_0)} \sum_{j=1}^{k_\varepsilon} W_j L^e(x_j, \omega'_j), \quad j = 1, \dots, k_\varepsilon, \quad (5)$$

where the weights are defined as follows

$$W_0 = 1, \quad W_j = W_{j-1} \frac{K(x_j, \omega'_j)}{p(x_j, \omega'_j)}, \quad j = 1, \dots, k_\varepsilon.$$

Theorem 1. *The expected value of the estimator (5) is equal to the functional (4) in case when we replace the radiance L with its iterative solution L_{k_ε} , i.e.*

$$E(\xi_{k_\varepsilon}[g]) = J_g(L_{k_\varepsilon}).$$

Proof. Taking into account the definition for an expected value of a random variable and the Neumann series of the Eq.(3), we obtain:

$$\begin{aligned} E(\xi_{k_\varepsilon}[g]) &= E \left(\frac{g(x_0, \omega'_0)}{p_0(x_0, \omega'_0)} \sum_{j=1}^{k_\varepsilon} W_j L^e(x_j, \omega'_j) \right) = \\ &= \sum_{j=1}^{k_\varepsilon} E \left(\frac{g(x_0, \omega'_0)}{p_0(x_0, \omega'_0)} W_j L^e(x_j, \omega'_j) \right) = \sum_{j=1}^{k_\varepsilon} (g, \mathbb{I} K^j L^e) = (g, L_{k_\varepsilon}) = J_g(L_{k_\varepsilon}). \end{aligned}$$

This completes the proof.

It is clear that when $k_\varepsilon \rightarrow \infty$ (this is the case of a infinite Markov chain) the MC estimator (5) evaluates the functional (4).

Using N independent samples of the estimator (5) we can compute the mean value:

$$\bar{\xi}_{k_\varepsilon}[g] = \frac{1}{N} \sum_{i=1}^N (\xi_{k_\varepsilon}[g])_i \xrightarrow{\text{Prob}} J_g(L_{k_\varepsilon}) \approx J_g(L), \quad (6)$$

where $\xrightarrow{\text{Prob}}$ means stochastic convergence as $N \rightarrow \infty$; L_{k_ε} is the iterative solution obtained by the Neumann series of Eq.(2).

The root mean square deviation is defined by the relation (see [11]):

$$E(\xi_{k_\varepsilon}[g] - J_g(L))^2 = \text{Var}(\xi_{k_\varepsilon}[g]) + (E(\xi_{k_\varepsilon}[g]) - J_g(L))^2,$$

where $\text{Var}(\xi_{k_\varepsilon}[g])$ is the variance of the MC estimator. Hence

$$E(\bar{\xi}_{k_\varepsilon}[g] - J_g(L))^2 = \frac{\text{Var}(\bar{\xi}_{k_\varepsilon}[g])}{N} + (J_g(L) - E(\xi_{k_\varepsilon}[g]))^2 \leq \frac{d_0}{N} + c_3 \varepsilon^2 = \mu^2, \quad (7)$$

where μ is the desired error; d_0 is upper boundary of the variance; ε is a priori given small parameter, and c_3 is the constant. Therefore, if the variance is bounded, the optimal order of the quantities N and ε must be $N = O(\mu^{-2})$ and $\varepsilon = O(\mu)$. In order to estimate the variance let us introduce notation:

$$\theta_j = \frac{g(x_0, \omega'_0)}{p_0(x_0, \omega'_0)} W_j L^e(x_j, \omega'_j),$$

$$p(x_0, \omega'_0, x_1, \omega'_1, \dots, x_j, \omega'_j) = p_0(x_0, \omega'_0) p(x_1, \omega'_1) \dots p(x_j, \omega'_j), \quad j = 1, 2, \dots.$$

Theorem 2. *Let us choose the initial density and transition density in the following way:*

$$p_0(x_0, \omega'_0) = \frac{|g(x_0, \omega_0)|}{\int_S \int_{\Omega_{x_0}} g(x_0, \omega_0) dx_0 d\omega_0}, \quad p(x, \omega') = \frac{K(x, \omega')}{\int_{\Omega_x} K(x, \omega') d\omega'}. \quad (8)$$

Then the variance of the MC estimator (5) is bounded.

Proof. It is enough to prove that $E(\xi_{k_\varepsilon}^2[g])$ is bounded. Taking into account the following inequality (see [10])

$$\left(\sum_{j=1}^{\infty} \theta_j \right)^2 \leq \sum_{j=1}^{\infty} \frac{t^{-j}}{1-t} \theta_j^2, \quad 0 < t < 1,$$

we have

$$\begin{aligned} Var(\xi_{k_\varepsilon}[g]) &\leq E(\xi_{k_\varepsilon}^2[g]) = E \left(\sum_{j=1}^{k_\varepsilon} \theta_j \right)^2 \leq E \left(\sum_{j=1}^{\infty} \theta_j \right)^2 \leq \\ &\sum_{j=1}^{\infty} \frac{t^{-j}}{1-t} E(\theta_j^2) = \sum_{j=1}^{\infty} \frac{t^{-j}}{1-t} \int_{S_{x_0}} \int_{\Omega_{x_0}} \int_{\Omega_{x_1}} \dots \int_{\Omega_{x_j}} \frac{g^2(x_0, \omega'_0)}{p_0^2(x_0, \omega'_0)} \times \\ &W_j^2(L^e)^2(x_j, \omega'_j) p(x_0, \omega'_0, x_1, \omega'_1, \dots, x_j, \omega'_j) dx_0 d\omega_0 \dots d\omega_j. \end{aligned}$$

Taking in account the choice of the densities we obtain

$$\begin{aligned} Var(\xi_{k_\varepsilon}[g]) &\leq \sum_{j=1}^{\infty} \frac{t^{-j}}{1-t} \left(\int_{S_{x_0}} \int_{\Omega_{x_0}} \int_{\Omega_{x_1}} \dots \int_{\Omega_{x_j}} g(x_0, \omega'_0) \times \right. \\ &K(x_0, \omega'_0) \dots K(x_j, \omega'_j) L^e(x_j, \omega'_j) dx_0 d\omega_0 \dots d\omega_j \left. \right)^2 \leq \sum_{j=1}^{\infty} \frac{t^{-j}}{1-t} g_*^2 (L^e)^2 (q^2)^j, \end{aligned}$$

where $g_* = \|g\|_{L_\infty}$. If we choose, $1 > t > q$, then we have

$$Var(\xi_{k_\varepsilon}[g]) \leq g_*^2 (L^e)^2 \frac{q^2}{(1-t)(t-q^2)}.$$

This completes the proof.

The choice Eq.(8) of the initial and transition densities leads to a reduction of the variance. We note that this choice is used in practice and it is very closely to the importance sampling strategy for variance reduction. The density functions (8) are called "almost optimal" densities [12]. In other cases when is not possible the choice (8), but the densities are chosen to be proportional to the main contribution from the kernel of the rendering equation.

When $g(x, \omega) = \frac{\chi_P(x)}{|P|} \delta(\omega)$ the MC estimator (5) evaluates the mean value of the radiance \bar{L}_P over pixel area (1). In this case, we can take $\varepsilon = 1/(2.2^8)$ because the primary colours in the RGB colour system are presented by 8-bit numbers.

4 Summary and Issues for Future Work

The presented MC estimator evaluates the rendering equation derived from the Cook-Torance illumination model. It is proved that the variance of this estimator is bounded when we use almost optimal initial and transition densities. We obtain condition for balancing of systematic and stochastic errors. The advantages of the studied MC approach lie in the direct estimation of the functional value in fixed phase space points. Also, this approach is easy for parallel realizations over MIMD (multiple instruction - multiple data) architectures and Grid's. Finally, the future research of the MC approach under consideration for Cook-Torance model could be developed in the following directions: 1. Development of computational MC algorithms for creation of photorealistic images. 2. Investigation of the computational complexity of the algorithms for different materials. 3. Creation of parallel MC algorithms for high performance and Grid computing.

References

1. Blinn, James F., Models of Light Reflection for Computer Synthesized Pictures, *Computer Graphics*, vol. 11, No. 2, pp. 192-198, (1977).
2. Cook, Robert L. and Torrance, Kenneth E., A Reflectance Model for Computer Graphics, *ACM Transactions on Graphics*, vol. 1, No. 1, pp. 7-24, (1982).
3. Hall, Roy A. and Greenberg, Donald P., A Testbed for Realistic Image Synthesis, *IEEE Computer Graphics and Applications*, vol. 3, No. 8, pp. 10-20, (1983).
4. He, Xiao D., Torrance, Kenneth E., Sillion, Francois and Greenberg, Donald P., A Comprehensive Physical Model for Light Reflection, *Computer Graphics*, vol. 25, No. 4, pp. 175-186, (1991).
5. Kajiya, J. T., The Rendering Equation, *Computer Graphics*, vol. 20, No. 4, pp. 143-150, *Proceedings of SIGGRAPH'86*, (1986).
6. Keller, Alexander, Quasi-Monte Carlo Methods in Computer Graphics: The Global Illumination Problem, *Lectures in Applied Mathematics*, vol. 32, pp. 455-469, (1996).
7. Phong, Bui Tuong, Illumination for Computer Generated Pictures, *Communication of the ACM*, June, vol. 18, No. 6, pp. 311-317, (1975).

8. Szirmay-Kalos, Laszlo, Monte-Carlo Methods in Global Illumination, Script in WS of 1999/2000, <http://www.fsz.bme.hu/szirmay/script.pdf>
9. Ward, Gregory, Measuring and modeling anisotropic reflection Computer Graphics, vol. 26 No. 2, pp. 265–272, (1992).
10. Gurov, T.V., Whitlock, P.A.: An efficient backward Monte Carlo estimator for solving of a quantum kinetic equation with memory kernel, *Math. & Comp. in Simul.* **60** (2002) pp. 85–105.
11. Mikhailov, G.A.: New Monte Carlo Methods with Estimating Derivatives. Utrecht, The Netherlands, (1995).
12. I. Dimov, Minimization of the probable error for some Monte Carlo methods. *Proc. of the Summer School on Math. Modeling and Sci. Computations, 23-28.09.1990, Albena, Bulgaria* (Publ. House of the Bulg. Acad. Sci., Sofia, 1991) 159–170.
13. Penzov, A. A., A Data Base Containing Spectral Data of Materials for Creating Realistic Images, Part 1: Theoretical Background, MTA SZTAKI, Report CG-1, Budapest, (1992).
14. Penzov, A. A., Shading and Illumination Models in Computer Graphics - a literature survey, MTA SZTAKI, Research Report CG-4, Budapest, (1992).